ACS APPLIED MATERIALS & INTERFACES

Research Article

www.acsami.org

Beneficial Role of Copper in the Enhancement of Durability of Ordered Intermetallic PtFeCu Catalyst for Electrocatalytic Oxygen Reduction

Balamurugan Arumugam,[†,‡] Takanori Tamaki,[‡,†] and Takeo Yamaguchi*[,‡,†]

[†]Kanagawa Academy of Science and Technology, 4259 Nagatsuta, Midori-Ku, Yokohama, Japan 226-8503

[‡]Chemical Resources Laboratory, Tokyo Institute of Technology, R1-17, 4259 Nagatsuta, Midori-Ku, Yokohama, Japan 226-8503

Supporting Information

ABSTRACT: Design of Pt alloy catalysts with enhanced activity and durability is a key challenge for polymer electrolyte membrane fuel cells. In the present work, we compare the durability of the ordered intermetallic face-centered tetragonal (fct) PtFeCu catalyst for the oxygen reduction reaction (ORR) relative to its counterpart bimetallic catalysts, i.e., the ordered intermetallic fct-PtFe catalyst and the commercial catalyst from Tanaka Kikinzoku Kogyo, TKK-PtC. Although both fct catalysts initially exhibited an ordered structure and mass activity approximately 2.5 times higher than that of TKK-Pt/C, the presence of Cu at the ordered intermetallic fct-PtFeCu catalyst led to a significant enhancement in durability compared to that of the ordered intermetallic fct-PtFe catalyst. The ordered intermetallic fct-PtFeCu catalyst retained more than 70% of its mass activity and electrochemically active surface area (ECSA) over 10 000 durability cycles carried out at 60 °C. In contrast, the ordered intermetallic fct-PtFe catalyst maintained only about 40% of its activity. The temperature of the durability experiment is also shown to be important: the catalyst was more severely degraded at 60 °C than at room temperature. To obtain insight into the observed enhancement in durability of fct-PtFeCu catalyst, a postmortem analysis of the ordered intermetallic fct-PtFeCu catalyst was carried out using scanning transmission electron microscopy-energy dispersive X-ray spectroscopy (STEM-EDX) line scan. The STEM-EDX line scans of the ordered intermetallic fct-PtFeCu catalyst over 10 000 durability cycles showed a smaller degree of Fe and Cu dissolution from the catalyst. Conversely, large dissolution of Fe was identified in the ordered intermetallic fct-PtFe catalyst, indicating a lesser retention of Fe that causes the destruction of ordered structure and gives rise to poor durability. The enhancement in the durability of the ordered intermetallic fct-PtFeCu catalyst is ascribed to the synergistic effects of Cu presence and the ordered structure of catalyst.

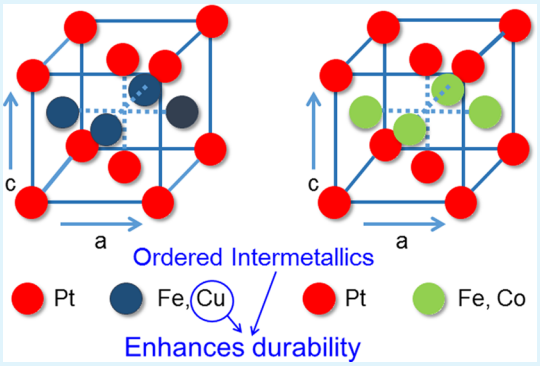

KEYWORDS: *ordered intermetallic, ORR, durability, PtFeCu catalyst, polymer electrolyte fuel cell*

1. INTRODUCTION

The emission of greenhouse gases from automobiles as well as in energy production by combustion of fossil fuels is of growing concern because of global warming. This has led to a deployment of an enormous scientific effort to find an alternative conversion device for sustainable energy production.[1−5] Polymer electrolyte membrane fuel cells (PEMFCs) are devices that can convert chemical energy into electrical energy with zero emission of greenhouse gases.[3−5] Oxygen reduction reaction (ORR) is a cathodic half-cell reaction that underlies the PEMFC operation; however, this reaction is sluggish even when platinum catalysts are used in PEMFCs. Consequently, a huge Pt catalyst loading is required to overcome the sluggish kinetics. To reduce Pt loading and to enhance the ORR activity by a factor of 2−5 over that of the pure platinum catalyst, the transition metals (M = Fe, Cu, Co, Ni, etc.,) have been alloyed with Pt to form PtM alloys.[3−18] The enhancement in ORR activity of PtM alloy catalysts has been attributed to various mechanisms such as the bifunctional mechanism, downshifting of the *d* band center, and electronic and geometric effects.[6−9,19] Despite the demonstration of the improved PtM alloy catalysts for the ORR activity, the inevitable dissolution of transition metals under the strongly acidic operating conditions of PEMFCs hinders their large-scale commercialization because of the decreased activity and hence limited durability of the catalyst.[20,21] Although immense efforts have been devoted to overcome the durability issues of the PtM alloy catalysts, so far the attained durability performance is either unsatisfactory or associated with difficulties in implementation in actual PEMFCs operations.[4,5,16,17,21,22]

The concept of the ordered intermetallic PtM alloy catalyst has been developed in the quest to mitigate the dissolution of

Received: April 11, 2015
Accepted: July 10, 2015
Published: July 10, 2015

DOI: 10.1021/acsami.5b03137
ACS Appl. Mater. Interfaces 2015, 7, 16311−16321

the M metals and therefore enhance the PtM alloy catalyst durability. The ordered intermetallic PtM alloy catalyst has a well-defined composition, and its atoms are arranged in an ordered manner (Scheme 1) in contrast to that of the PtM alloy catalyst, termed disordered face-centered cubic (fcc)-PtM alloy catalyst, where the composition is ill-defined and the atomic arrangement is disordered. In addition to enhanced durability, the favorable structural features of the ordered intermetallic PtM catalyst enable an enhancement of the ORR activity relative to that of the disordered PtM alloy catalyst.[23−34] These effects were demonstrated using several intermetallic PtM alloy catalysts such as PtCo,[23] PtFe,[24−28] PtCu,[29−31] and PtCr.[32] We have also examined the activity and durability of the ordered intermetallic fct-PtFeCo catalysts in our previous study.[33] The enhancement in durability of ordered intermetallic catalyst was attributed to the leaching tolerance of transition (M) metals from the ordered catalysts; this helped to preserve the ordered structure and gave rise to an enhanced durability.[23,30,33]

Scheme 1. Structure of (A) Ordered Intermetallic fct-PtFeCu Catalyst and (B) Ordered Intermetallic fct-PtFeCo Catalyst

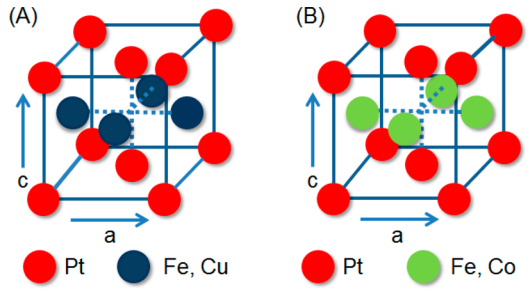

In this work, we evaluate the durability of the ordered intermetallic face-centered tetragonal (fct)-PtFeCu (Scheme 1A), the ordered intermetallic fct-PtFe, and a copper-free ternary-ordered intermetallic fct-PtFeCo catalyst (Scheme 1B). The synergistic effect of the ordered structure and Cu with higher standard redox potential is expected to enhance the durability of the catalyst. Electrochemical characterization and the postmortem analysis using scanning transmission electron microscopy-energy dispersive X-ray spectroscopy (STEM-EDX) line scan were carried out. On the basis of the combination of the electrochemical results and postmortem analysis, we suggest a mechanism for the enhanced durability.

2. EXPERIMENTAL SECTION

2.1. Catalyst Preparation and Characterization. Metallic precursors such as hexachloroplatinic acid for platinum (Pt), vinyl ferrocene for Iron (Fe), cobalt(II) acetate tetrahydrate for cobalt (Co), and copper(II) acetate monohydrate for copper (Cu) were received from Wako Chemicals. The catalysts were prepared using the solid-state impregnation technique. Briefly, to obtain 500 mg of 40 wt % PtFeCu/C catalyst the following procedure was used. A 404.8 mg aliquot of hexachloroplatinic acid (for Pt), 82.8 mg of vinyl ferrocene (for Fe), and 78 mg of copper acetate tetrahydrate (for Cu) were added into 300 mg of Ketjen Black Carbon (KBC). These metallic precursors were mixed uniformly with KBC and then ground well to attain a smooth and dark fine powder. This mixture was then converted into paste by adding about 2 mL of isopropyl alcohol (IPA) and then again ground well to obtain a fine powder. The powder was then reduced in the presence of 20% H_2 with N_2 as carrier gas in a tube furnace for 4 h. The ordered intermetallic fct-PtFeCu/C catalyst was obtained by annealing at 800 °C, whereas the disordered fcc-PtFeCu/C catalyst was generated by annealing at ≤700 °C. Following a similar procedure, the ordered intermetallic fct-PtFeCo catalyst and ordered intermetallic fct-PtFe catalyst were prepared by annealing at 800 °C. The quantities of metal precursors used for the ordered intermetallic fct-PtFeCo catalyst were as follows: 410.2 mg of hexachloroplatinic acid (for Pt), 84 mg of vinyl ferrocene (for Fe), and 98.65 mg of cobalt acetate tetra hydrate (for Co) with 300 mg of KBC. For the ordered intermetallic PtFe catalyst the following quantities were used: 405 mg of hexachloroplatinic acid (for Pt) and 165.7 mg of vinyl ferrocene (for Fe) with 300 mg of KBC.

Inductively coupled plasma-atomic emission spectroscopy (ICP-AES, Shimadzu-ICPS 8100) was used to determine the catalyst composition. The catalyst was first dissolved in aqua regia and then diluted to a concentration of 50 ppm for the analysis. In addition, thermogravimetric analysis (TGA, PerkinElmer Pyris1 TGA) was carried out to estimate the metal loading on KBC. The catalyst metal composition, total metal loading, and Pt loading data on the carbon support are presented in Tables 1 and 2. The X-ray diffraction (XRD) data were collected for 2θ = 10−90° with a scan rate of 3°/min on a RINT2100 (Rigaku Co. Ltd. Japan) diffractometer using Cu Kα line (λ= 1.5418 Å, 40 kV, 40 mA). STEM-EDX line-scan measurements were carried out using an HD-2700 C_S-corrected STEM (Hitachi High Technologies Corporation).The convergence semiangle was 32 mrad, and the collection semiangle was 70−370 mrad. To measure the STEM-EDX line scan of ordered intermetallic PtFeCu catalyst, the samples were coated on the molybdenum grid (Mo grid) to ensure that the copper signal did not arise from the grid. TEM images were observed via a JEM-2010 field emission transmission electron microscope (JEOL, Japan). Rotating disk electrode (RDE) and cylic voltammetry (CV) measurements were taken using an HSV-100 automatic polarization system (Hokuto Denko,Tokyo), whereas the durability experiments were carried out using an HSV-7000 automatic polarization system (Hokuto Denko,Tokyo) instrument.

Table 1. Lattice Parameters, ICP-AES Composition, and Metal Loading for PtFeCu Catalyst at Different Annealing Temperatures and for the TKK-PtC Catalyst

	lattice parameter (Å)				
temperature (°C)	a	c	metal composition, ICP	total metal/Pt loading (%)	Pt loading on the electrode surface (μg cm^{-2})
TKK-PtC[a]	3.912			45.8	17.2
400	3.875		$Pt_{53}Fe_{23}Cu_{24}$	40.1/31.4	11.9
600	3.862		$Pt_{54}Fe_{25}Cu_{21}$	41.5/33.5	12.3
700	3.831		$Pt_{47}Fe_{27}Cu_{25}$	45.5/34.1	12.8
800	3.810	3.674	$Pt_{52}Fe_{22}Cu_{26}$	46.7/36.3	13.5

[a]As received.

2.2. Electrochemical Measurements. For the preparation of catalyst ink, 18.5 mg of catalyst was mixed into 25 mL of 24% of IPA solution and 100 μL of Nafion (5 wt %, Aldrich), and the mixture was sonicated until a well-dispersed ink was obtained. Then, 10 μL of ink was drop coated on a mirror-polished glassy-carbon (0.196 cm^2) electrode and then dried under an alcohol atmosphere. The data for the final Pt loading on the glassy-carbon disk electrode surface are summarized in Tables 1 and 2 for all the catalysts. In all the electrochemical and durability experiments, 0.1 M $HClO_4$ solution was used as an electrolyte. Reversible hydrogen electrode (RHE) and Pt wire were used as reference and counter electrodes, respectively.

Prior to measurements of the initial CV cycles, the modified electrode (working electrode) was cleaned in N_2-saturated 0.1 M $HClO_4$ solution by cycling the potential between 0.05 and 1.2 V (RHE) at the scan rate of 50 mV s^{-1} until a reproducible voltammogram was obtained. The durability of these catalyst was

DOI: 10.1021/acsami.5b03137
ACS Appl. Mater. Interfaces 2015, 7, 16311−16321

Table 2. Lattice Parameters, ICP-AES Composition and Metal Loading Results for Ordered Intermetallic fct-PtFeCu, Ordered Intermetallic fct-PtFe Catalyst, and Ordered Intermetallic fct-PtFeCo Catalyst[a]

	lattice parameter (Å)				
catalyst	a	c	metal composition, ICP	total metal/Pt loading (%)	Pt loading on the electrode surface (μg cm^{-2})
fct-$Pt_{50}Fe_{25}Cu_{25}$	3.814	3.674	$Pt_{52}Fe_{22}Cu_{26}$	46.7/36.3	13.5
fct-$Pt_{50}Fe_{50}$	3.808	3.673	$Pt_{49}Fe_{51}$	46.0/35.0	13.1
fct-$Pt_{50}Fe_{25}Co_{25}$	3.825	3.712	$Pt_{48}Fe_{25}Co_{27}$	47.0/36.0	13.3

[a]All the catalysts were synthesized by annealing at 800 °C.

examined in load cycle test according to revised protocol of Fuel Cell Commercialization Conference of Japan (FCCJ)[35] at room temperature or 60 °C. The load cycle durability test of the catalyst was examined by applying square wave cycling, 0.6 V for 3 s and 1.0 V for 3 s in accordance with the FCCJ protocol. The 60 °C temperature of the durability experiments was harsher than in our previous study where durability was evaluated at room temperature. In this work, both temperatures, i.e., room temperature and 60 °C, were employed in the durability experiments for comparison. The durability experiment at 60 °C was carried out three times for each catalyst. RDE polarization curve and CV were recorded at room temperature. RDE polarization curve was reordered at the scan rate of 20 mV s^{-1} from negative to positive potential for both N_2 and O_2 saturated solutions. The background-subtracted or mass-transport-corrected LSV curve was obtained by subtraction of LSV of O_2 from N_2.

3. RESULTS AND DISCUSSION

To find the optimum temperature for the phase transition of the disordered fcc into the ordered fct for the PtFeCu catalyst, the samples were annealed at different temperatures ranging from 400 to 800 °C, and their XRD patterns are shown in Figure 1. It can be seen that an increase in the annealing

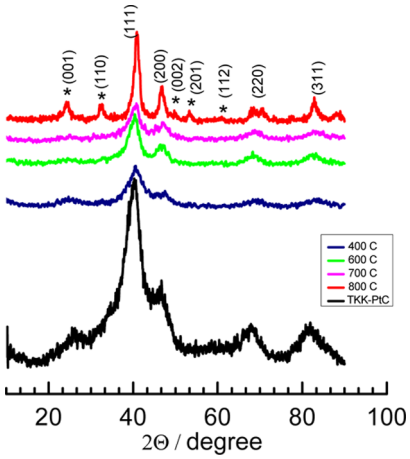

Figure 1. XRD patterns of TKK-PtC catalyst and PtFeCu catalyst obtained at different annealing temperatures. * indicates superlattice phases.

temperature shifts the diffraction peaks to higher 2θ values for the PtFeCu catalyst with respect to those of the fcc-Pt catalyst (commercial TKK-PtC catalyst). This indicates that insertion of Fe and Cu atoms into the Pt lattice is present and leads to the shortening of the lattice parameter and Pt−Pt distance, confirming the formation of alloy.[5,8,9] The lattice parameter values for these catalysts are shown in Table 1. The diffraction peaks observed up to 700 °C for the PtFeCu catalyst are the characteristic peaks of the Pt fcc structure. Hence, these catalysts are hereafter denoted as disordered fcc-PtFeCu catalyst. Intriguingly, the catalyst annealed at 800 °C shows two additional sharp reflections at 2θ of 24.30° for (001) and 32.40° for (110) that are not found in the disordered fcc-PtFeCu catalyst. These reflections correspond to superlattice peaks, confirming the formation of the ordered intermetallic fct-PtFeCu catalyst.[23−34,36,37] In general, equiatomic amounts of Pt and M (M = Fe, Co, and Cu) yield the $L1_0$ (CuAu) or fct phase structure with an alternation of the Pt and M atoms along the (001) direction. Hence, it is also expected that alternating planes of Pt and Fe/Cu will be present in the ordered intermetallic fct-PtFeCu catalyst, in agreement with our previous report.[33] The lattice parameters for the ordered intermetallic fct-PtFeCu catalyst are calculated by considering the (001) and (110) peaks[38] and the resulting values are given in Table 1.

The ORR activities of these catalysts were examined, and their mass activity (I_m), ECSA and specific activities (I_s) are presented in Figure 2. I_m and I_s at 0.9 V were calculated according to literature.[39] ECSA was calculated from the peak area of hydrogen desorption from ca. 0.08 to 0.4 V, by assuming the charge for removing a monolayer hydrogen on Pt to be 210 μC cm^{-2}. A monotonic rise is observed for both I_m (Figure 2a) and I_s (Figure 2b) after increasing the annealing temperature of the catalyst above 600 °C, whereas ECSA decreases above 600 °C. This result suggests that although the particle size increases with the increase in the temperature the effect of the size on the mass activity is limited under the experimental condition of this study. The increase in the activity with the increase in the temperature may be correlated with the shortening of Pt−Pt distance (Table 1) with the formation of alloy and the transformation to ordered fct structure. The I_m of the ordered intermetallic fct-PtFeCu catalyst prepared at 800 °C is about 0.53 A mg_{Pt}^{-1}; this value is fairly comparable with the reported literature values.[3] The I_m of the ordered intermetallic fct-PtFeCu catalyst is 2.5 times higher than that of the TKK-PtC catalysts (0.2 A mg_{Pt}^{-1}). Conversely, the I_m values of the disordered fcc-PtFeCu catalysts (prepared at 400−700 °C) falls to between 0.35 and 0.4 A mg_{Pt}^{-1}, 1.3−1.5 times smaller than that of the ordered intermetallic fct-PtFeCu catalysts. A similar enhancement in mass activity was reported for the ordered intermetallic PtCo,[6] PtCu,[7] PtFe,[8] and PtFeCo[33] catalysts including in our work, as compared to their corresponding disordered catalyst. Furthermore, the I_s of the ordered intermetallic fct-PtFeCu catalyst (1.35 mA cm_{Pt}^{-2}) is 4 times higher than that of the TKK-PtC catalyst (0.34 mA cm_{Pt}^{-2}). The enhancement in I_m and I_S of the ordered intermetallic fct-PtFeCu catalyst can be ascribed to the electronic effect of a decrease in the *d*-band center and the lowering of binding energies of adsorbates as well as to strained lattice effects.[6,40,41]

The main objective of the present work is to examine the beneficial role of Cu at the ordered intermetallic fct-PtFeCu catalyst for the enhancement of durability relative to that of the ordered intermetallic fct-PtFe catalyst and the ordered

DOI: 10.1021/acsami.5b03137
ACS Appl. Mater. Interfaces 2015, 7, 16311−16321

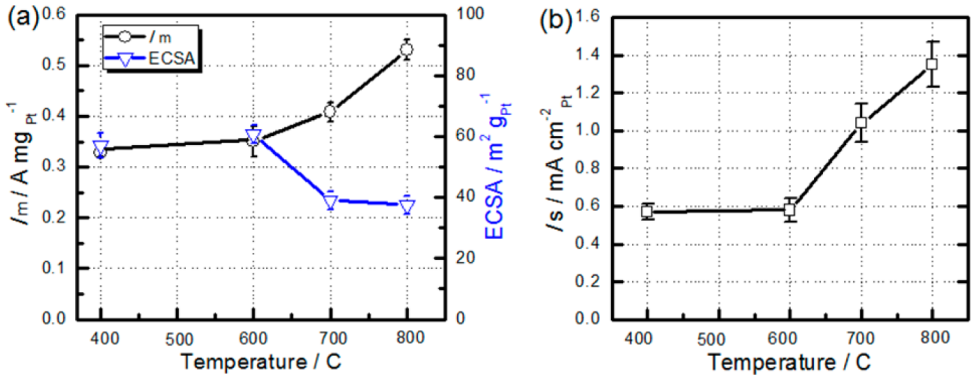

Figure 2. (a) I_m and ECSA and (b) I_s for PtFeCu catalyst at different annealing temperature. I_m and I_s are calculated at 0.9 V vs RHE. Error bars denote standard deviations of three independent experiment.

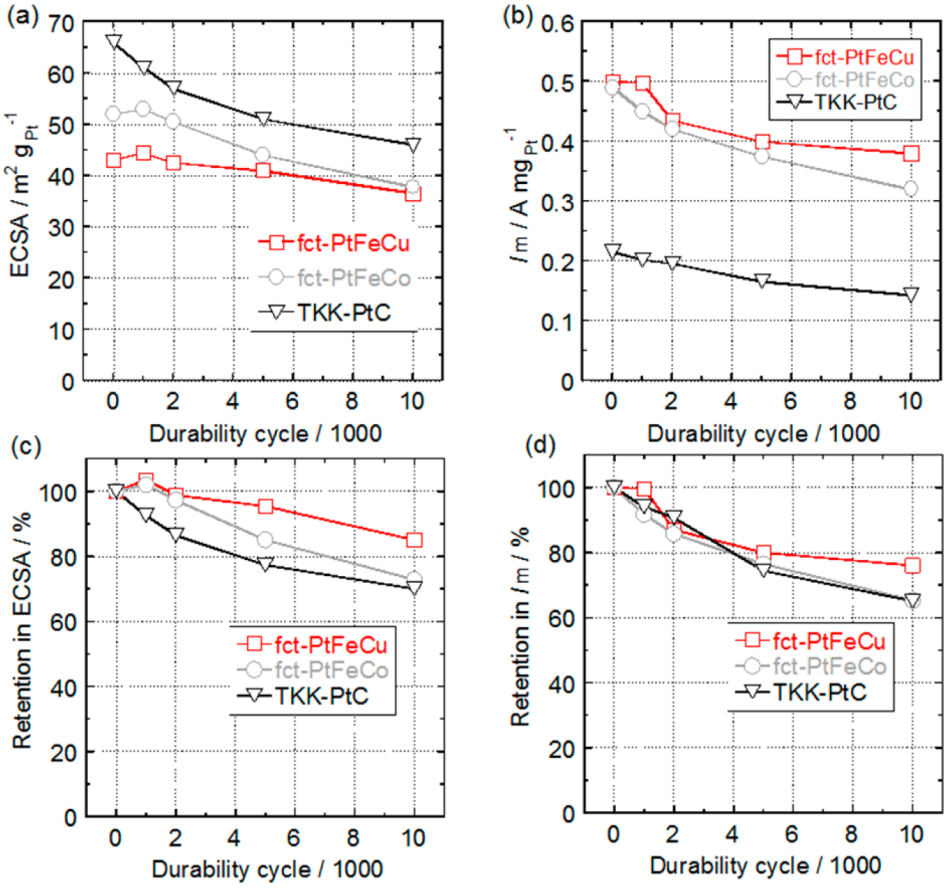

Figure 3. (a) ECSA, (b) mass activity, (c) retention in ECSA, and (d) retention in mass activity for different numbers of durability cycles at room temperature.

intermetallic fct-PtFeCo catalyst. The ordered intermetallic fct-PtFeCo catalyst was used as the control ternary catalyst to demonstrate the beneficial role of Cu in the ordered intermetallic fct-PtFeCu catalyst. The XRD patterns of the three ordered intermetallic catalysts are shown in Supporting Information Figure S1. Similar to the case of the ordered intermetallic fct-PtFeCu catalyst, the ordered intermetallic fct-PtFeCo catalyst and the ordered intermetallic fct-PtFe catalyst also show XRD reflections including the (110) and (001) superlattice reflections that are the evidence for the formation of an ordered intermetallic structure.[6−8,33] The lattice parameter values for these catalysts are given in Table 2. The calculated values are lower than those for the TKK-PtC catalyst, indicating lattice contraction.

First, we examined the durability of ordered intermetallic fct-PtFeCu and ordered intermetallic fct-PtFeCo catalyst at room temperature in a load cycle test region according to FCCJ protocol, and their results are compared with those of the TKK-PtC catalyst. The CVs and RDE voltammogram at different durability cycles of these catalysts are shown in Supporting Information Figure S2. The ECSA, I_m, and retention in ECSA and I_m at different potential durability cycles for these catalysts are shown in Figure 3. It can be seen that the loss in ECSA and I_m for the ordered intermetallic fct-PtFeCu catalyst is significantly less over 10 000 durability cycles than those of

DOI: 10.1021/acsami.5b03137
ACS Appl. Mater. Interfaces 2015, 7, 16311−16321

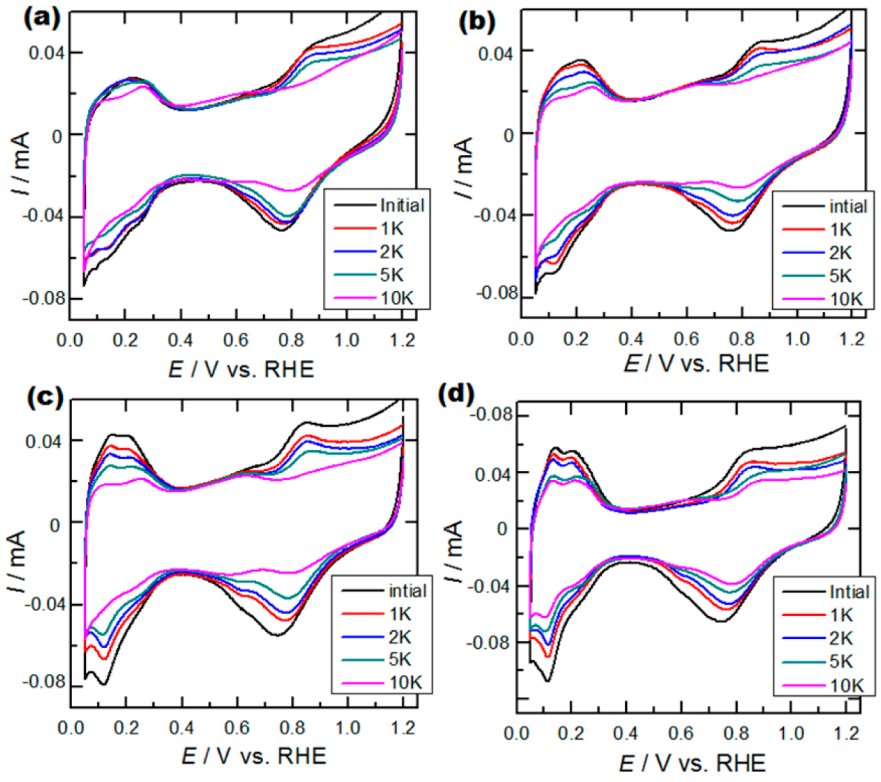

Figure 4. CVs at different potential durability cycles at 60 °C for (a) ordered intermetallic fct-PtFeCu catalyst, (b) ordered intermetallic fct-PtFe catalyst, (c) ordered intermetallic fct-PtFeCo catalyst, and (d) TKK-PtC catalyst.

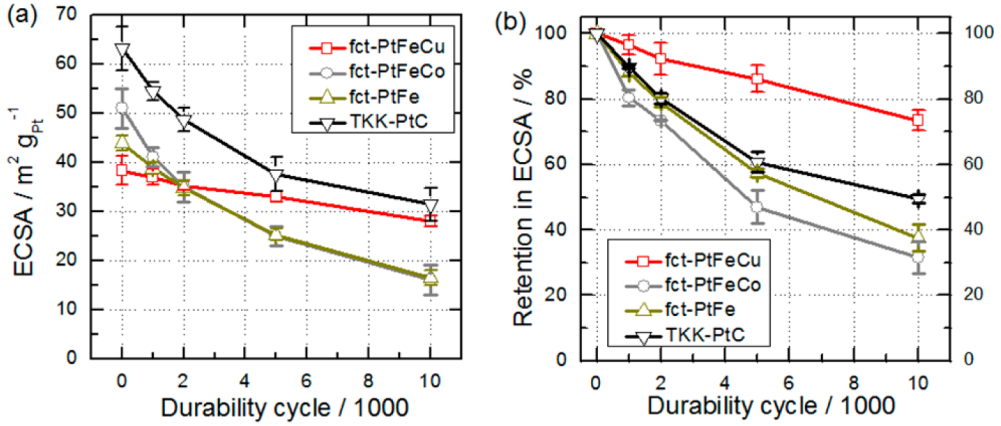

Figure 5. (a) ECSAs and (b) retention in ECSAs for catalysts for different numbers of durability cycles at 60 °C. Error bars denote standard deviations of three independent experiments.

the other catalysts; it retained 85% of ECSA and 75% of its initial I_m, as shown in Figure 3. In the case of ordered intermetallic fct-PtFeCo catalyst, the retention in ECSA and I_m are found to be 84 and 77%, respectively, over 5000 durability cycles, and the TKK-PtC catalyst retains 76% of both ECSA and I_m over 5000 durability cycles. These results almost agree with our previous report wherein the durability experiments were carried out at room temperature.[33] At 10 000 durability cycles, both ordered intermetallic fct-PtFeCo and TKK-PtC catalysts retain 70% of ECSA and 65% of initial mass activity.

Furthermore, the durability test of these catalysts was evaluated at 60 °C to examine a more accelerated condition because degradation of Pt and Pt−M alloy catalysts is more severe than at room temperature. The CVs and ECSA at different potential durability cycles are shown in Figures 4 and 5, respectively. For the ordered intermetallic fct-PtFeCu catalyst (Figure 4a), the decrease in the magnitude of CV current and the change in ECSAs are negligibly small over 5000 potential durability cycles. Then, a gradual decrease in durability after 10 000 cycle is observed, describing the slow dissolution of Fe and Cu atoms from the catalyst. After 10 000 cycles, more than 75% of ECSAs are retained as shown in Figure 5b. In contrast, the ordered intermetallic fct-PtFe catalyst shows a significant decrease in the magnitude of CV current (Figure 4b) from the initial cycle to the 5000 cycles, with the decrease continuing until 10 000 cycles. At 10 000 cycles, the ordered intermetallic fct-PtFe catalyst retains only 40% of ECSAs (Figure 5b). The significant decrease in ECSA for the ordered intermetallic PtFe catalyst was also reported previously by Gotton et al. and Xia et al.[27−29] The control

DOI: 10.1021/acsami.5b03137
ACS Appl. Mater. Interfaces 2015, 7, 16311−16321

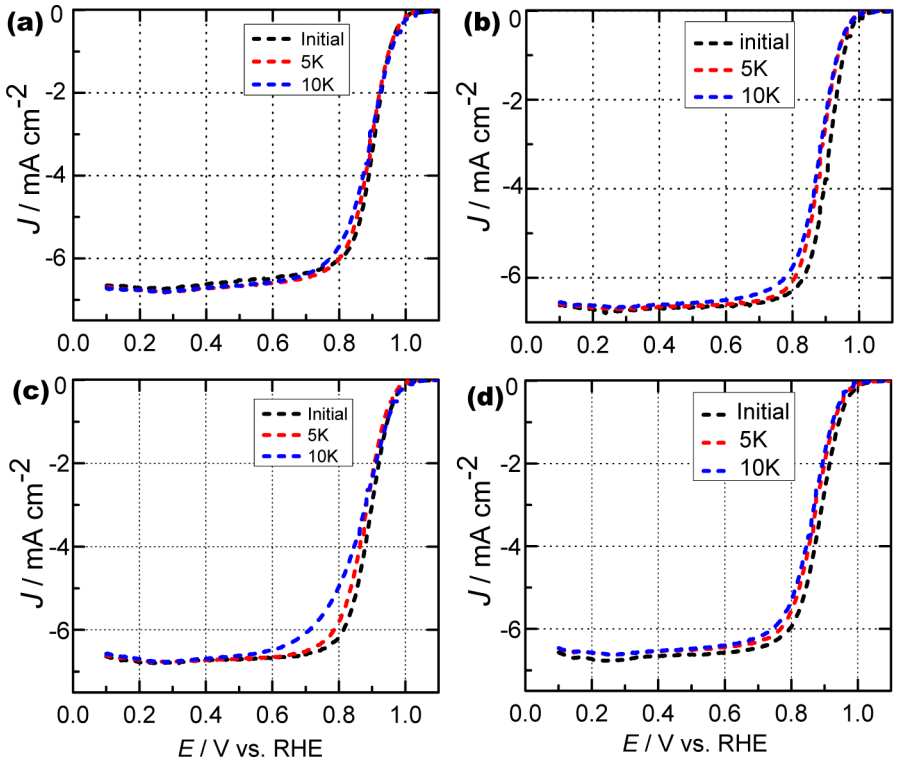

Figure 6. ORR polarization curves at different potential durability cycles at 60 °C for (a) ordered intermetallic fct-PtFeCu catalyst, (b) ordered intermetallic fct-PtFe catalyst, (c) ordered intermetallic fct-PtFeCo catalyst, and (d) TKK-PtC catalyst.

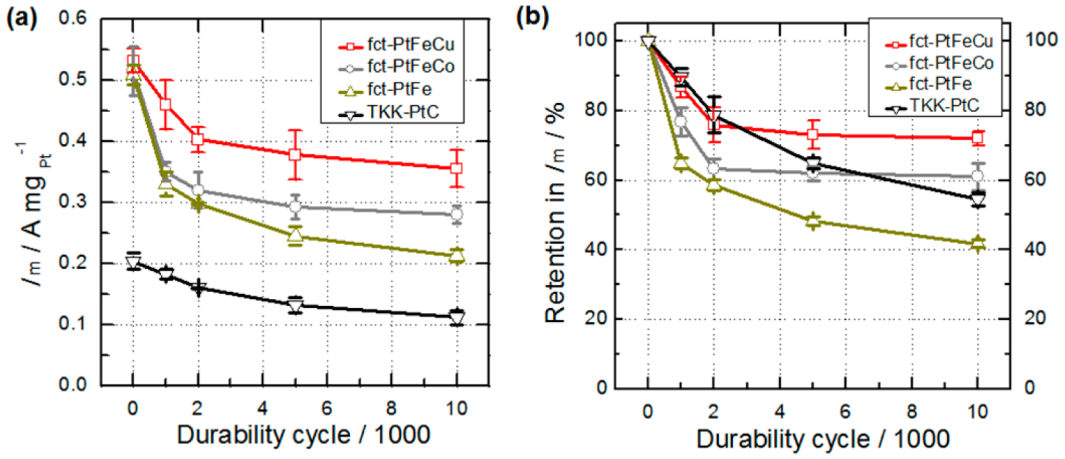

Figure 7. (a) Mass activity and (b) retention in mass activity for catalysts for different numbers of durability cycles at 60 °C. Error bars denote standard deviations of three independent experiments.

catalyst, i.e., the ordered intermetallic fct-PtFeCo catalyst, exhibits a similar decrease in the magnitude of CV current (Figure 4c) with retention of around 30% of ECSA (Figure 5b). This finding reveals that a rapid dissolution of Fe from the ordered intermetallic fct-PtFe catalyst and of Fe/Co from the ordered intermetallic fct-PtFeCo catalysts occurred, despite the ordered intermetallic structure of these catalysts. Such a rapid dissolution of Fe and Fe/Co from their respective catalysts can lead to the appearance of bulk Pt-like behavior, causing significant loss in ECSA values.[7] For comparison, the durability results of TKK-PtC catalyst are also incorporated, and the potential-dependent CVs are shown in Figure 4d. The retention in ECSAs is 50% over 10 000 cycles, consistent with the results reported in previous work.[42] The loss in ECSAs could be explained as the electrochemical Ostwald ripening.[43] Moreover, in the present work we observe a sharp decline in the durability (retention of ECSAs) at 60 °C for the ordered intermetallic fct-PtFeCo catalyst as compared to its durability at room temperature (Figure 3 and our previous report[33]). This is also the case for TKK-PtC catalyst. The observed difference could be correlated with the changes in the temperature because the rate of the dissolution of M metals from PtM alloy and Pt dissolution and redeposition (electrochemical Ostwald ripening) at PtC catalyst is faster at higher temperature than at lower temperature (room temperature), leading to a rapid appearance of bulk Pt-like behavior and a consequent decrease of the ECSA.[5,44,45] Furthermore, it was found that in our previous work the ordered intermetallic PtFeCo catalyst

DOI: 10.1021/acsami.5b03137
ACS Appl. Mater. Interfaces 2015, 7, 16311−16321

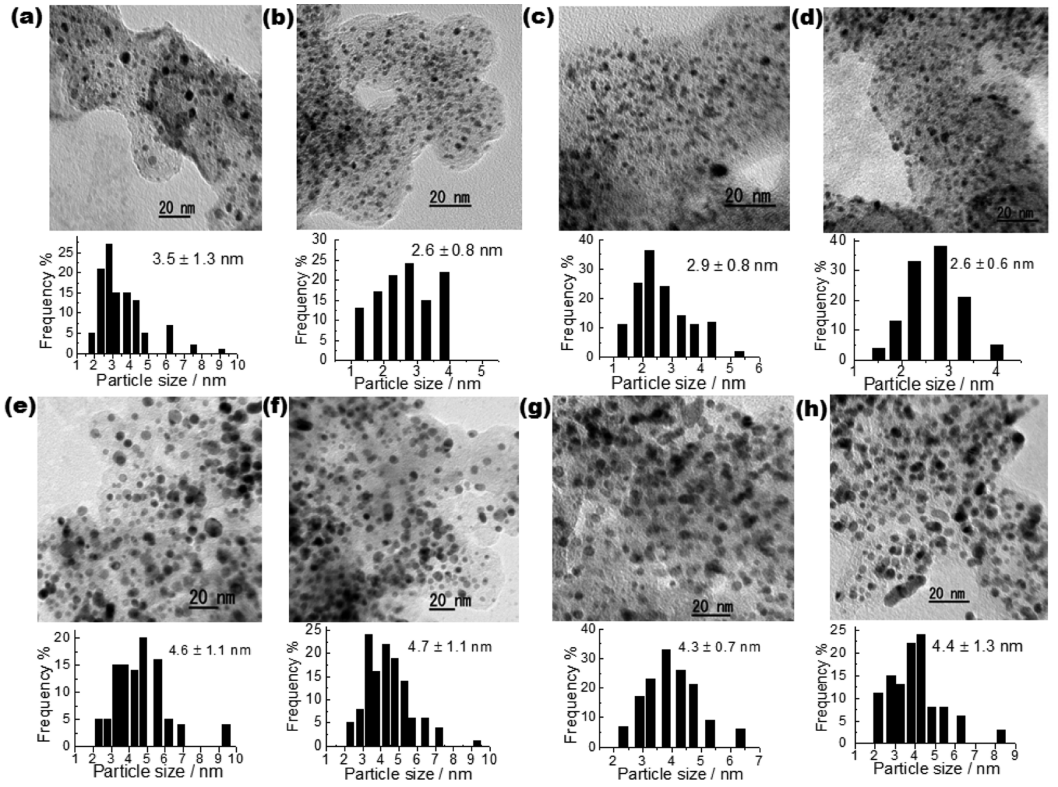

Figure 8. TEM images of (a and e) ordered intermetallic fct-PtFeCu catalyst, (b and f) ordered intermetallic fct-PtFe catalyst, (c and g) ordered intermetallic fct-PtFeCo catalyst, and (d and h) TKK-PtC catalyst. Images a–d are for the initial state, and images e–h are after 10 000 cycles at 60 °C.

displayed enhanced durability with respect to TKK-PtC catalyst under a membrane electrode assembly (MEA) condition whose working temperature was 80 °C.[46] The observed trend in durability is different for RDE and MEA. This may be because dissolution and diffusion of M metals from the PtM alloy catalyst could be faster in RDE than in MEA. In RDE, the local environment around the catalysts is hot $HClO_4$ acid solution, whereas in MEA, the catalysts surrounded by the polymer electrolyte are basically in the gaseous phase.

The durability cycle-dependent RDE voltammogram and mass activities for these catalysts are shown in Figures 6 and 7, respectively. The durability experiment was carried out using the ordered intermetallic catalysts, fct-PtFuCu, fct-PtFe, and fct-PtFeCo, with similar initial mass activity. The retention in mass activity of fct-PtFeCu is higher than that of the other two catalysts, fct-PtFe and fct-PtFeCo. This higher retention in mass activity of fct-PtFeCu agree with the higher retention in ECSA of the catalyst. The degradation in the half-wave potential (Figure 6a, $E_{1/2}$) is only 15 mV over 10 000 durability cycles with 70% retention (Figure 7b) of its initial I_m for the ordered intermetallic fct-PtFeCu catalyst. Nonetheless, the shift in the $E_{1/2}$ value for the ordered intermetallic fct-PtFe catalyst is significantly higher, i.e., 30 mV with 40% retention of its initial I_m. Furthermore, degradation of the $E_{1/2}$ value is around 26 mV for the intermetallic fct-PtFeCo catalysts with 60% retention of its initial I_m. We also show the RDE voltammogram at potential durability cycles for TKK-PtC catalyst in Figure 6d with its mass activity depicted in Figure 7. TKK-PtC catalyst retains only 55% of its initial mass activity. At 10 000 durability cycles, I_m of ordered intermetallic fct-PtFeCu catalyst (0.36 A mg_{Pt}^{-1}) is 2.8 times higher than that of the TKK-PtC catalyst (0.12 A mg_{Pt}^{-1}). From these durability results, it is evident that the ordered intermetallic fct-PtFeCu catalyst displayed enhanced durability with around 70% retention of initial I_m and ECSA over 10 000 durability cycles, implying a small deterioration of the ordered intermetallic fct-PtFeCu catalyst.[31−34]

Postmortem analysis was carried out to obtain insight into the origin of the durability enhancement exhibited by the ordered intermetallic fct-PtFeCu catalyst. Figure 8 compares TEM images obtained initially and after 10 000 durability cycles along with the particle size distribution histograms and particle sizes; the percent increases in particle size over 10 000 durability cycles are summarized in Table 3. The growth in particle size is significantly less over 10 000 durability cycles for the ordered intermetallic fct-PtFeCu catalyst than for the other catalysts. We found here that the particle size increases from the initial value of 3.5 ± 1.3 to 4.6 ± 1.5 nm after at 10 000 durability cycles, corresponding to an increase in the particle size of only 34%. This small growth in particle size is consistent

Table 3. Average Particle Size Initially, After 10 000 Durability Cycles at 60 °C, and Percentage of Increase in Particle Size over 10 000 Durability Cycles for All the Catalysts

	crystal size (nm)		
catalyst	initial	@10000 cycle at 60 °C	increase in crystal size (%)
TKK-PtC	2.6 ± 0.6	4.4 ± 1.3	69
fct-$Pt_{50}Fe_{25}Cu_{25}$	3.5 ± 1.3	4.6 ± 1.1	34
fct-$Pt_{50}Fe_{50}$	2.6 ± 0.8	4.7 ± 1.1	81
fct-$Pt_{50}Fe_{25}Co_{25}$	2.9 ± 0.8	4.3 ± 0.7	50

DOI: 10.1021/acsami.5b03137
ACS Appl. Mater. Interfaces 2015, 7, 16311−16321

with maximum retention in ECSAs. Conversely, for the ordered intermetallic fct-PtFe and fct-PtFeCo catalysts, much larger increases in particle size of 85 and 50%, respectively, are observed. For the TKK-PtC catalyst, a similar 70% growth in particle size is observed. The observed trend in particle growth is consistent with the measured retention in ECSA.

We then used the STEM-EDX line-scan measurements to reveal the enhancement in durability at the ordered intermetallic fct-PtFeCu through comparison with the results for the ordered intermetallic fct-PtFe catalysts. Although ICP-AES is suitable to measure bulk composition of the catalysts, the amount of catalysts loaded on the RDE is small; thus, quantitative evaluation of the composition after the durability test is difficult using ICP-AES. The STEM-EDX line-scan measurements were carried out for the initial state and for three particles of the ordered intermetallic fct-PtFeCu and fct-PtFe catalysts after 2000 and 10 000 durability cycles. All the line-scans are shown in Figures S3−S8, and the typical results for fct-PtFeCu and fct-PtFe are depicted in Figures 9 and 10,

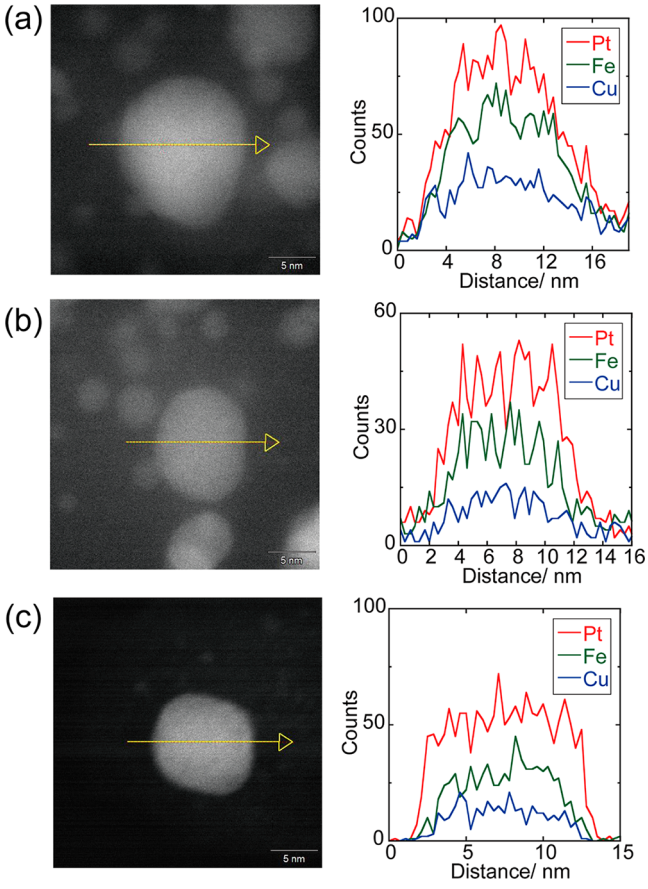

Figure 9. HAADF-STEM images (left) and STEM-EDX line-scans (right) for ordered intermetallic fct-PtFeCu catalyst. The images were taken after (a) the initial cycle, (b) 2000 cycles, and (c) 10 000 durability cycles at 60 °C.

respectively. To further understand the changes in atomic composition, the STEM-EDX line-scan results obtained at the center of the particles were used to calculate the average ratios of the counts of Fe/Pt and Cu/Pt for the ordered intermetallic fct-PtFeCu catalyst and of Fe/Pt for the ordered intermetallic fct-PtFe catalyst. The average ratios of the counts are summarized in Table 4. Figure 9a shows the STEM-EDX line

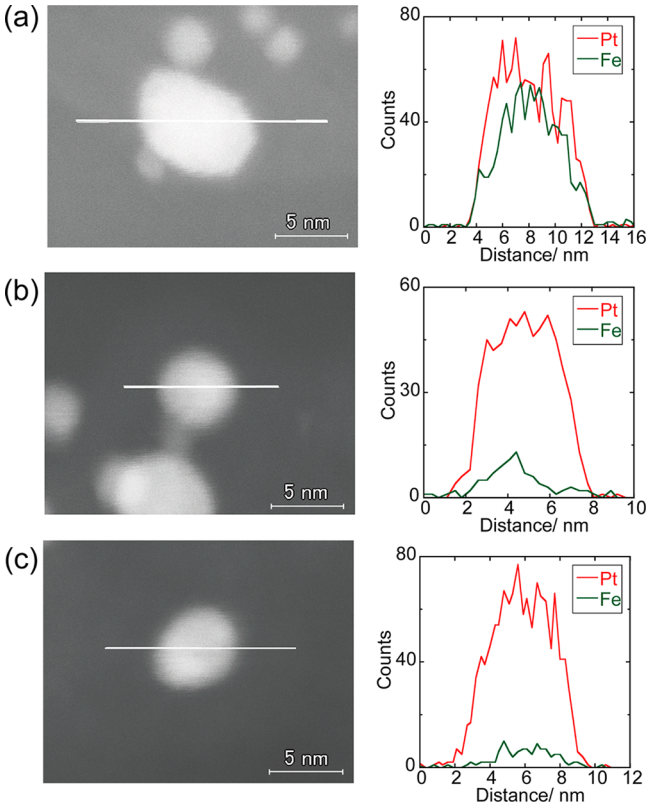

Figure 10. HAADF-STEM images (left) and STEM-EDX line-scans (right) for ordered intermetallic fct-PtFe catalyst. The images were taken after (a) the initial cycle, (b) 2000 cycles, and (c) 10 000 durability cycles at 60 °C.

scan of the ordered intermetallic fct-PtFeCu catalyst particle at the initial state. We draw two conclusions from the examination of the line scan shown in Figure 9a: (1) Fe and Cu atoms atom are distributed uniformly throughout the particle, unlike Pt which shows a higher concentration at the center of the particle. (2) Fe, Cu, and Pt atoms intermixed at both edges of the particle. These observations imply that the particle exhibits a graded structure composition without a discrete changeover, i.e., no core−shell type structure is formed. Although earlier reports demonstrated the formation of core−shell-type PtM alloy catalyst at higher temperature, they also revealed that core−shell type formation depended on the temperature and also the bulk ratio of alloying components.[7] After 2000 durability cycles (Figure 9b), the line-scan profile feature is similar to that observed initially, although a minor loss in Fe and Cu is identified. From the initial state until after 2000 durability cycles, the average ratios of counts of Fe/Pt and Cu/Pt decrease slightly from 0.68 to 0.54 for Fe/Pt and from 0.39 to 0.28 for Cu/Pt relative to the data obtained at 2000 cycles. The corresponding loss is about 20% for Fe/Pt and 28% for Cu/Pt. This small loss may be caused by the dissolution of the surface or near-surface Fe and Cu metals from the catalysts.[7,23] Interestingly, the decline in average ratios of counts of Fe/Pt and Cu/Pt is negligibly low at 10 000 durability cycles (Figure 9c) as compared to that at 2000 cycles, demonstrating negligible dissolution of Fe and Cu atoms during this period of cycles. The losses in the average ratios of counts are 25% for Fe/Pt and 30% for Cu/Pt over 10 000 durability cycles, indicating that most of the Fe and Cu metal is well-preserved in the catalyst over 10 000 durability cycles; alternatively, the high

DOI: 10.1021/acsami.5b03137
ACS Appl. Mater. Interfaces 2015, 7, 16311−16321

Table 4. Average Ratios of Counts of Fe/Pt, Cu/Pt and Co/Pt around the Center of the Particle at Different Durability Cycles

catalyst	fct-PtFeCu						fct-PtFe			fct-PtFeCo[a]				
	Fe/Pt			Cu/Pt			Fe/Pt			Fe/Pt		Co/Pt		
	initial	2000	10000	initial	2000	10000	initial	2000	10000	initial	5000	ini	5000	
average ratios of counts[b]	0.68 ± 0.03	0.54 ± 0.07	0.52 ± 0.01	0.39 ± 0.07	0.28 ± 0.07	0.25 ± 0.03	0.74 ± 0.03	0.30 ± 0.09	0.16 ± 0.04	0.31	0.17	0.31	0.14	
retention (%)		79	75		72	64		40	22		55		45	

[a]Average ratios of Fe/Pt and Co/Pt of the ordered intermetallic fct-PtFeCo catalyst were acquired from our previous work of STEM-EDX line scan.[33] The durability experiments for fct-PtFeCo were carried out at room temperature, whereas those for fct-PtFeCu and fct-PtFe were carried out at 60 °C. [b]The results on three particles were used to calculate average ± standard deviation for fct-PtFeCu and fct-PtFe.

subsurface concentration of Fe and Cu atom retain the benefit of good contact with Pt over 10 000 durability cycles.[7,47] In the case of ordered intermetallic fct-PtFe catalyst, the uniform distribution of Fe and Pt around the particle with high counts of Pt at the center of particles is detected for the initial state (Figure 10a). As predicted, a significant drop in the average ratios of counts of Fe/Pt is observed after 2000 cycles (Figure 10b) compared to that at the initial cycle (Figure 10a) and decreases more between 2000 and >10 000 durability cycles. After 10 000 durability cycles, the loss in Fe/Pt counts is 78%, indicating a significant dissolution of Fe from the catalyst that leads to poor subsurface concentration of Fe after 10 000 durability cycles. This trend, i.e., dissolution of Fe from fct-PtFe catalyst, is different from that observed in previous research by Sun's group where the fully ordered fct-FePt catalyst showed a very small loss of Fe content after 20 000 durability cycles.[28] There may be two main differences that can explain this opposite trend: the degree of ordered structure and the temperature of the durability experiment. The catalysts prepared in this study may differ in the degree of ordered structure from the fully ordered fct-FePt catalyst prepared by Sun's group. The latter point, the temperature of the durability test, is shown to be important in this study; although the degradation experiment at room temperature has been usually employed previously, this study revealed that degradation of the catalysts is more accelerated at 60 °C than at room temperature as shown from the comparison between Figure 3 and Figures 5 and 7. The degradation of fct-PtFe catalyst in this study is further evidence of the observed poor durability caused by the activity of PtM alloy catalyst on the concentration of M metals on the subsurface.[5,7,47,48] Conversely, for the ordered intermetallic fct-PtFeCu catalyst, the maximum extent of Fe and Cu atoms is retained, and fewer Fe and Cu are dissolved. This shows that the maximum extent of the ordered structure can be preserved in the ordered intermetallic fct-PtFeCu catalyst and that a slight chance of transition of the ordered fct structure into a disordered fcc structure may be ignored. A similar observation was made for the ordered intermetallic fct-PtFeCo catalyst in our previous study where durability experiments were carried out at room temperature and where the ordered intermetallic fct-PtFeCo catalyst preserved most of the ordered structure despite the loss in the average ratios of Fe/Pt and Co/Pt (50 and 45%, respectively, after 5000 durability cycles).[33] Therefore, it is certain that the retention of the maximum Fe and Cu content and hence maximum extent of ordered structure was sustained for the ordered intermetallic fct-PtFeCu catalyst, enabling maximum activity over 10 000 durability cycles (Figure 7).

On the basis of these findings and the postmortem analysis, a possible mechanism for the enhanced durability at the ordered intermetallic fct-PtFeCu catalyst is presented. In general, the dissolution of transition metals (M) from the PtM alloy is inevitable in PEMFCs because of their highly acidic working environment. The dissolution of M from the alloy depends on the standard redox potential of the individual M and also the structural arrangements of the PtM alloy catalysts.[16,17] The standard redox potentials of Fe, Cu, and Pt are −0.44, 0.34, and 1.19 V, respectively, which means that Fe undergoes oxidation more easily than Cu and Pt. STEM-EDX line scan revealed that both Fe and Cu were retained after 10 000 durability cycles. The presence of Cu is the most likely impediment for Fe dissolution in this catalyst. This is similar to the results of previous work that have shown that a metal element with a

DOI: 10.1021/acsami.5b03137
ACS Appl. Mater. Interfaces 2015, 7, 16311−16321

higher standard redox potential metal element can inhibit the dissolution of an element with a lower redox potential.[16,17,49] For instance, Adzic et al. found that the PtPdAu alloy catalyst displayed enhanced durability over that of the PtPd alloy catalyst and observed that Au increases the oxidation resistance of Pd.[17] Additionally, the electronic effect caused by structural ordering also contributes to enhanced durability of the catalyst.[22] The synergistic effect of the ordered structure and Cu with higher standard redox potential retained Fe and Cu in the catalyst; this helps to retain the ordered structure in the ordered intermetallic fct-PtFeCu catalyst, accounting for the enhanced durability in ECSA and mass activity. The effect of Cu in the ordered fct structure on the enhancement of durability should be investigated in more detail using, e.g., quantum calculation. On the basis of these results, we illustrated comparative particle structure over 10 000 durability cycles, as shown in Figure 11.

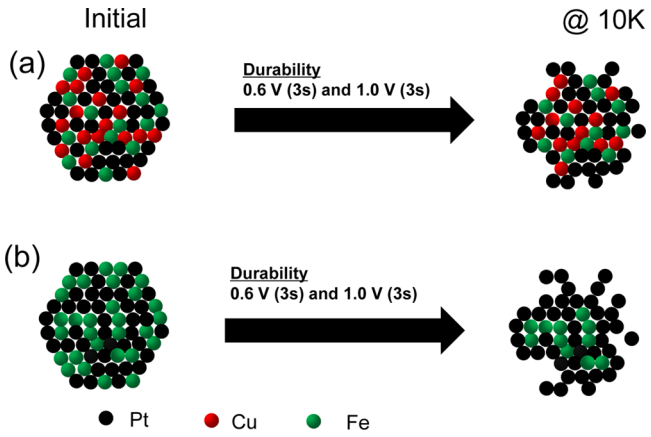

Figure 11. Schematic illustration of particle before and after 10 000 durability cycles for (a) ordered intermetallic fct-PtFeCu catalyst and (b) ordered intermetallic fct-PtFe catalyst.

3. CONCLUSIONS

We demonstrated that the presence of copper in the ordered intermetallic fct-PtFeCu catalyst enhances its durability for the ORR. The copper-containing catalyst retained more than 70% of mass activity and ECSA, whereas the ordered intermetallic fct-PtFe catalyst showed a significant loss of activity. The TKK-PtC catalyst also retained only about 50% of its initial mass activity and ECSA over 10 000 durability cycles. In addition, the temperature of the durability experiment was shown to be important: the catalysts were more severely degraded at 60 °C than at room temperature. The mass activity of the ordered intermetallic fct-PtFeCu catalyst was enhanced by more than twofold with respect to that of TKK-PtC catalyst, both at the initial state and after 10 000 durability cycles. The enhancement in durability was attributed to the hindered dissolution of Fe and Cu from the catalyst as shown using the STEM-EDX line scans; this facilitated the retention of the ordered catalyst structure.

■ ASSOCIATED CONTENT

Supporting Information

XRD patterns of ordered intermetallic fct-PtFe and fct-PtFeCo catalysts. CVs and ORR polarization curves at different potential durability cycles at room temperature. All the HAADF-STEM images and STEM-EDX line-scans for ordered intermetallic fct-PtFeCu and fct-PtFe catalysts at initial, 2000, and 10 000 durability cycles at 60 °C. The Supporting Information is available free of charge on the ACS Publications website at DOI: 10.1021/acsami.5b03137.

■ AUTHOR INFORMATION

Corresponding Author

*E-mail:yamag@titech.ac.jp.

Notes

The authors declare no competing financial interest.

■ REFERENCES

(1) Kim, D.; Resasco, J.; Yu, Y.; Asiri, A. M.; Yang, P. Synergistic Geometric and Electronic Effects for Electrochemical Reduction of Carbon Dioxide using Gold−Copper Bimetallic Nanoparticles. *Nat. Commun.* **2014**, *5*, 4948.

(2) Gratzel, M. Photoelectrochemical Cells. *Nature* **2001**, *414*, 338−344.

(3) Debe, M. K. Electrocatalyst Approaches and Challenges for Automotive Fuel Cells. *Nature* **2012**, *486*, 43−51.

(4) Chen, C.; Kang, Y.; Huo, Z.; Zhu, Z.; Huang, W.; Xin, H. L.; Snyder, J.D.; Li, D.; Herron, J. A.; Mavrikakis, M.; Chi, M.; More, K. L.; Li, Y.; Markovic, N. M.; Somorjai, G. A.; Yang, P.; Stamenkovic, V. R. Highly Crystalline Multimetallic Nanoframes with Three-Dimensional Electrocatalytic Surfaces. *Science* **2014**, *343*, 1339−1343.

(5) Yano, H.; Song, J. M.; Uchida, H.; Watanabe, M. Temperature Dependence of Oxygen Reduction Activity at Carbon-Supported Pt_XCo (X = 1, 2, and 3) Alloy Catalysts Prepared by the Nanocapsule Method. *J. Phys. Chem. C* **2008**, *112*, 8372−8380.

(6) Stamenkovic, V. R.; Fowler, B.; Mun, B. S.; Wang, G.; Ross, P. N.; Lucas, C. A.; Markovic, N. M. Improved Oxygen Reduction Activity on Pt_3Ni (111) via Increased Surface Site Availability. *Science* **2007**, *315*, 493−497.

(7) Stamenkovic, V. R.; Mun, B. S.; Mayrhofer, K. J. J.; Ross, P. N.; Markovic, N. M. Effect of Surface Composition on Electronic Structure, Stability and Electrocatalytic Properties of Pt-transition Metal Alloys: Pt-skin versus Pt-skeleton Surfaces. *J. Am. Chem. Soc.* **2006**, *128*, 8813−8819.

(8) Kakade, B. A.; Wang, H.; Tamaki, T.; Ohashi, H.; Yamaguchi, T. Enhanced Oxygen Reduction Reaction by Bimetallic CoPt and PdPt Nanocrystals. *RSC Adv.* **2013**, *3*, 10487−10496.

(9) Okaya, K.; Yano, H.; Uchida, H.; Watanabe, M. Control of Particle Size of Pt and Pt Alloy Electrocatalysts Supported on Carbon Black by the Nanocapsule Method. *ACS Appl. Mater. Interfaces* **2010**, *2*, 888−895.

(10) Zhang, C.; Hwang, S. Y.; Trout, A.; Peng, Z. Solid-State Chemistry-Enabled Scalable Production of Octahedral Pt−Ni Alloy Electrocatalyst for Oxygen Reduction Reaction. *J. Am. Chem. Soc.* **2014**, *136*, 7805−7808.

(11) Carpenter, M. K.; Moylan, T. E.; Kukreja, R. K.; Atwan, M. H.; Tessema, M. M. Solvothermal Synthesis of Platinum Alloy Nanoparticles for Oxygen Reduction Electrocatalysis. *J. Am. Chem. Soc.* **2012**, *134*, 8535−8542.

(12) Alia, S. M.; Pylypenko, S.; Neyerlin, K. C.; Cullen, D. A.; Kocha, S. S.; Pivovar, B. S. Platinum-Coated Cobalt Nanowires as Oxygen Reduction Reaction Electrocatalysts. *ACS Catal.* **2014**, *4*, 2680−2686.

(13) Strasser, P.; Koh, S.; Anniyev, T.; Greeley, J.; More, K.; Yu, C.; Liu, Z.; Kaya, S.; Nordlund, D.; Ogasawara, H.; Toney, M. F.; Nilsson, A. Lattice-strain Control of the Activity in Dealloyed Core-shell Fuel Cell Catalysts. *Nat. Chem.* **2010**, *2*, 454−460.

(14) Srivastava, R.; Mani, P.; Hahn, N.; Strasser, P. Efficient Oxygen Reduction Fuel Cell Electrocatalysis on Voltammetrically de-alloyed Pt−Cu−Co Nanoparticles. *Angew. Chem., Int. Ed.* **2007**, *46*, 8988−8991.

(15) Wang, J. X.; Inada, H.; Wu, L.; Zhu, Y.; Choi, Y.; Liu, P.; Zhou, W. P.; Adzic, R. R. Oxygen Reduction on Well-Defined Core_Shell

DOI: 10.1021/acsami.5b03137
ACS Appl. Mater. Interfaces 2015, 7, 16311−16321

Nanocatalysts: Particle Size, Facet, and Pt Shell Thickness Effects. *J. Am. Chem. Soc.* **2009**, *131*, 17298−17302.
(16) Kang, Y.; Snyder, J.; Chi, M.; Li, D.; More, K. L.; Markovic, N. M.; Stamenkovic, V. R. Multimetallic Core/Interlayer/Shell Nanostructures as Advanced Electrocatalysts. *Nano Lett.* **2014**, *14*, 6361−6367.
(17) Sasaki, K.; Naohara, H.; Choi, Y.; Cai, Y.; Chen, W. F.; Liu, P.; Adzic, R. R. Highly Stable Pt Monolayer on PdAu Nanoparticle Electrocatalysts for the Oxygen Reduction Reaction. *Nat. Commun.* **2012**, *3*, 1115.
(18) Guldur, C.; Gunes, S. Carbon Supported Pt-based Ternary Catalysts for Oxygen Reduction in PEM Fuel Cells. *Catal. Commun.* **2011**, *12*, 707−711.
(19) Toda, T.; Igarashi, H.; Watanabe, M. Enhancement of the Electrocatalytic O_2 Reduction on Pt−Fe Alloys. *J. Electroanal. Chem.* **1999**, *460*, 258−262.
(20) Wang, C.; Markovic, N. M.; Stamenkovic, V. R. Advanced Platinum Alloy Electrocatalysts for the Oxygen Reduction Reaction. *ACS Catal.* **2012**, *2*, 891−898.
(21) Gan, L.; Heggen, M.; O'Malley, R.; Theobald, B.; Strasser, P. Understanding and Controlling Nanoporosity Formation for Improving the Stability of Bimetallic Fuel Cell Catalysts. *Nano Lett.* **2013**, *13*, 1131−1138.
(22) Kuttiyiel, K. A.; Sasaki, K.; Su, D.; Wu, L.; Zhu, Y.; Adzic, R. R. Gold-promoted Structurally Ordered Intermetallic Palladium Cobalt Nanoparticles for the Oxygen Reduction Reaction. *Nat. Commun.* **2014**, *5*, 5185.
(23) Wang, D.; Xin, H. L.; Hovden, R.; Wang, H.; Yu, Y.; Muller, D. A.; Disalvo, F. J.; Abruna, H. D. Structurally Ordered Intermetallic Platinum−Cobalt Core−shell Nanoparticles with Enhanced Activity and Stability as Oxygen Reduction Electrocatalysts. *Nat. Mater.* **2012**, *12*, 81−87.
(24) Kim, J.; Lee, Y.; Sun, S. H. Structurally Ordered FePt Nanoparticles and Their Enhanced Catalysis for Oxygen Reduction Reaction. *J. Am. Chem. Soc.* **2010**, *132*, 4996−4997.
(25) Li, X.; An, L.; Wang, X.; Li, F.; Zou, R.; Xia, D. Supported sub-5 nm Pt−Fe Intermetallic Compounds for Electrocatalytic Application. *J. Mater. Chem.* **2012**, *22*, 6047−6052.
(26) Chen, L.; Chan, M. C. Y.; Nan, F.; Bock, C.; Botton, G. A.; Mercier, P. H. J.; MacDougall, B. R. Compositional and Morphological Changes of Ordered PtxFey/C Oxygen Electroreduction Catalysts. *ChemCatChem* **2013**, *5*, 1449−1460.
(27) Li, X.; An, L.; Chen, X.; Zhang, N.; Xia, D.; Huang, W.; Chu, W.; Wu, Z. Durability Enhancement of Intermetallics Electrocatalysts via N-anchor Effect for Fuel Cells. *Sci. Rep.* **2013**, *3*, 3234 DOI: 10.1038/srep03234.
(28) Li, Q.; Wu, L.; Wu, G.; Su, D.; Lv, H.; Zhang, S.; Zhu, W.; Casimir, A.; Zhu, H.; Mendoza-Garcia, A.; Sun, S. New Approach to Fully Ordered fct-FePt Nanoparticles for Much Enhanced Electrocatalysis in Acid. *Nano Lett.* **2015**, *15*, 2468−2473.
(29) Bele, M.; Jovanovič, P.; Pavlišič, A.; Jozinović, B.; Zorko, M.; Rečnik, A.; Chernyshova, E.; Hočevar, S.; Hodnik, N.; Gaberščček, M. A Highly Active $PtCu_3$ Intermetallic Core−shell, Multilayered Pt-skin, Carbon Embedded Electrocatalyst Produced by a Scale-up Sol−gel Synthesis. *Chem. Commun.* **2014**, *50*, 13124−13126.
(30) Hodnik, N.; Jeyabharathi, C.; Meier, J. C.; Kostka, A.; Phani, K. L.; Rečnik, A.; Bele, M.; Hočevar, S.; Gaberščček, M.; Mayrhofer, K. J. J. Effect of Ordering of $PtCu_3$ Nanoparticle Structure on the Activity and Stability for the Oxygen Reduction Reaction. *Phys. Chem. Chem. Phys.* **2014**, *16*, 13610−13615.
(31) Wang, D.; Yu, Y.; Xin, H. L.; Hovden, R.; Ercius, P.; Mundy, J. A.; Chen, H.; Richard, J. H.; Muller, D. A.; DiSalvo, F. J.; Abruña, H. D. Tuning Oxygen Reduction Reaction Activity via Controllable Dealloying: A Model Study of Ordered Cu_3Pt/C Intermetallic Nanocatalysts. *Nano Lett.* **2012**, *12*, 5230−5238.
(32) Zou, L.; Li, J.; Yuan, T.; Zhou, Y.; Li, X.; Yang, H. Structural Transformation of Carbon-supported Pt_3Cr Nanoparticles from a Disordered to an Ordered Phase as a Durable Oxygen Reduction Electrocatalyst. *Nanoscale* **2014**, *6*, 10686−10692.
(33) Arumugam, B.; Kakade, B. A.; Tamaki, T.; Arao, M.; Imai, H.; Yamaguchi, T. Enhanced Activity and Durability for the Electroreduction of Oxygen at a Chemically Ordered Intermetallic PtFeCo catalyst. *RSC Adv.* **2014**, *4*, 27510−27517.
(34) Zhang, S.; Zhang, X.; Jiang, G.; Zhu, H.; Guo, S.; Su, D.; Lu, G.; Sun, S. H. Tuning Nanoparticle Structure and Surface Strain for Catalysis Optimization. *J. Am. Chem. Soc.* **2014**, *136*, 7734−7739.
(35) The Fuel Cell Commercialization Conference of Japan (FCCJ). http://fccj.jp/eng/index.html.
(36) Varanda, L. C.; Jafelicci, M. Self-Assembled FePt Nanocrystals with Large Coercivity: Reduction of the fcc-to-$L1_0$ Ordering Temperature. *J. Am. Chem. Soc.* **2006**, *128*, 11062−11066.
(37) Sun, S.; Murray, C. B.; Weller, D.; Folks, L.; Moser, M. Monodisperse FePt Nanoparticles and Ferromagnetic FePt Nanocrystal Superlattices. *Science* **2000**, *287*, 1989−1992.
(38) Koh, S.; Toney, M. F.; Strasser, P. Activity−stability Relationships of Ordered and Disordered Alloy Phases of Pt_3Co Electrocatalysts for the Oxygen Reduction Reaction (ORR). *Electrochim. Acta* **2007**, *52*, 2765−2774.
(39) Garsany, vY.; Baturina, O. A.; Swider-Lyons, K. E.; Kocha, S. S. Experimental Methods for Quantifying the Activity of Platinum Electrocatalysts for the Oxygen Reduction Reaction. *Anal. Chem.* **2010**, *82*, 6321−6328.
(40) Hyman, M. P.; Medlin, J. W. Effects of Electronic Structure Modifications on the Adsorption of Oxygen Reduction Reaaction Intermediates on Model Pt (111)-Alloy Surfaces. *J. Phys. Chem. C* **2007**, *111*, 17052−17060.
(41) Prabhudev, S.; Bugnet, M.; Bock, C.; Botton, G. A. Strained Lattice with Persistent Atomic Order in Pt_3Fe_2 Intermetallic Core-Shell Nanocatalysts. *ACS Nano* **2013**, *7*, 6103−6110.
(42) Higuchi, H.; Hayashi, K.; Chiku, M.; Inoue, H. Simple Preparation of Au Nanoparticles and Their Application to Au Core/Pt Shell Catalysts for Oxygen Reduction Reaction. *Electrocatalysis* **2012**, *3*, 274−283.
(43) Liu, Y.; Mustain, W. E. High Stability, High Activity Pt/ITO Oxygen Reduction Electrocatalysts. *J. Am. Chem. Soc.* **2013**, *135*, 530−533.
(44) Mitsushima, S.; Koizumi, Y.; Uzuka, S.; Ota, K. Dissolution of Platinum in Acidic Media. *Electrochim. Acta* **2008**, *54*, 455−460.
(45) Shao-Horn, Y.; Sheng, W. C.; Chen, S.; Ferreira, P. J.; Holby, E. F.; Morgan, D. Instability of Supported Platinum Nanoparticles in Low-Temperature Fuel Cells. *Top. Catal.* **2007**, *46*, 285−305.
(46) Tamaki, T.; Minagawa, A.; Arumugam, B.; Kakade, B. A.; Yamaguchi, T. Highly Active and Durable Chemically Ordered Pt-Fe-Co Intermetallics as Cathode Catalysts of Membrane-Electrode Assemblies in Polymer Electrolyte Fuel Cells. *J. Power Sources* **2014**, *271*, 346−353.
(47) Wang, C.; Chi, M.; Li, D.; Strmcnik, D.; van der Vliet, D.; Wang, G.; Komanicky, V.; Chang, K.; Paulikas, A. P.; Tripkovic, D.; Pearson, J.; More, K. L.; Markovic, N. M.; Stamenkovic, V. R. Design and Synthesis of Bimetallic Electrocatalyst with Multilayered Pt-Skin Surfaces. *J. Am. Chem. Soc.* **2011**, *133*, 14396−14403.
(48) Stephens, I. E. L.; Bondarenko, A. S.; Perez-Alonso, F. J.; Calle-Vallejo, F.; Bech, L.; Johansson, T. P.; Jepsen, A. K.; Frydendal, R.; Knudsen, B. P.; Rossmeisl, J.; Chorkendorff, I. Tuning the Activity of Pt(111) for Oxygen Electroreduction by Subsurface Alloying. *J. Am. Chem. Soc.* **2011**, *133*, 5485−5491.
(49) Tan, X.; Prabhudev, S.; Kohandehghan, A.; Karpuzov, D.; Botton, G. A.; Mitlin, D. Pt−Au−Co Alloy Electrocatalysts Demonstrating Enhanced Activity and Durability toward the Oxygen Reduction Reaction. *ACS Catal.* **2015**, *5*, 1513−1524.

DOI: 10.1021/acsami.5b03137
ACS Appl. Mater. Interfaces 2015, 7, 16311−16321